Research reports from Honors undergraduate students receiving support from the Shackouls Honors College via the Summer Research Fellowship

Summer 2020

Program Director:

Dr. Anastasia Elder

Edited by:

Alice Chandler

Table of Contents

Name: Hannah Douglas

Faculty Mentor: C. LaShan Simpson

Major: Biomedical Engineering

Department: Agricultural and Biological Engineering

Investigating the Role of Endothelial Cells in Vascular Calcification

Introduction: Vascular calcification (VC), which occurs when the medial and intimal layers of a vessel wall accrue calcium phosphate crystal deposits, is a colossal risk factor in regards to cardiovascular disease and mortality (Bardeesi et al., 2017; Yao et al., 2015). The myocardium, blood vessels, and cardiac valves are susceptible to the hydroxyapatite deposition of VC (Giachelli, 2009). Because the mineral deposits share properties of calcium in bone, it is known that similar mechanisms found in the formation of bone may contribute to the build-up of VC (Nahar-Gohad, Gohad, Tsai, Bordia, & Vyavahare, 2015). Furthermore, vascular smooth muscle cells (VSMC's) have been shown to transition into osteoblast-like cells through a phenotypic switch (Nahar-Gohad et al., 2015). Our previous lab work has shown that high blood serum phosphate levels contribute to phenotypic changes in VSMC's. Physiologically, endothelial cells (EC's) are in the first line of defense between blood serum and smooth muscle cells (SMC's). Uncovering the mechanism for the phenotypic switch of cells to calcified cells could lead to the development of a therapy or treatment in the future.

Proposed Research: In order to contribute to furthering the knowledge of the origins of VC, eventually leading to a therapeutic treatment, it was planned to investigate if endothelial cells play any role in the phenotypic switch of VSMC's. Cell culture, biochemical analysis techniques, and histology would be performed and learned in order to accomplish this goal.

Accomplishments: Because of the ongoing COVID-19 pandemic, our proposed research was unable to be executed as planned. However, we were able to remain productive. Our lab was invited to

write and publish a review article in the *journal of bioengineering*. The article we wrote, "Mechanisms of the Osteogenic Switch of Smooth Muscle Cells in Vascular Calcification: WNT Signaling, BMPs, Mechanotransduction, and EndMT," reviews VC and various pathways that contribute to its onset. I wrote and edited various sections of the paper, working with other members of our lab to efficiently complete the paper. Besides general edits, I wrote about WNT (one of the pathways leading to VC) inducers and inhibitors, obtained permission for the use of all utilized images, formatted the bibliography, and assisted in the writing of each section.

In addition to publishing the article, I began the trouble-shooting process of our lab's mechanical bioreactor. I learned how the machine works, as well as how to operate it. When we realized there was an error occurring, I examined the bioreactor and determined the problem to reside in the computer attached to the bioreactor and not the bioreactor itself. I maintained communications with the bioreactor's manufacturer in order to narrow down what the exact technical issue was, and we determined that the error was most likely within the computer's hardware.

Future Work: We plan to pursue the original proposed research experiment of determining the role of endothelial cells in VSMC phenotypic switch. Discovering their role in VC would bring scientists closer to devising a treatment for VC. In addition to the proposed research, we plan to continue repairing the bioreactor. Once repaired, we will utilize it to investigate the mechanical effects of high blood pressure on VSMC's in relation to VC. This second project also carries the potential to greatly impact future therapies and preventative treatments for VC.

Bibliography

Bardeesi, A. S. A., Gao, J., Zhang, K., Yu, S., Wei, M., Liu, P., & Huang, H. (2017, May 3). A novel role of cellular interactions in vascular calcification. *Journal of Translational Medicine*. BioMed Central Ltd. https://doi.org/10.1186/s12967-017-1190-z

Giachelli, C. M. (2009). The emerging role of phosphate in vascular calcification. *Kidney International*, *75*(9), 890–897. https://doi.org/10.1038/ki.2008.644

Nahar-Gohad, P., Gohad, N., Tsai, C. C., Bordia, R., & Vyavahare, N. (2015). Rat Aortic Smooth Muscle Cells Cultured on Hydroxyapatite Differentiate into Osteoblast-Like Cells via BMP-2–SMAD-5 Pathway. *Calcified Tissue International*, *96*(4), 359–369. https://doi.org/10.1007/s00223-015-9962-z

Yao, L., Sun, Y. T., Sun, W., Xu, T. H., Ren, C., Fan, X., … Wang, L. N. (2015). High phosphorus level leads to aortic calcification via β-catenin in chronic kidney disease. *American Journal of Nephrology*, *41*(1), 28–36. https://doi.org/10.1159/000370250

Conservation Prioritization Tool: Developing ecological criteria for guiding land conservation in the U.S. Gulf of Mexico Coastal Region

Madison Gnoose, Dr. Kristine Evans

Introduction

Decision-making in land conservation depends on apt data and detailed information that explains the benefits of conserving a particular landscape. This can be hard to accomplish, though, especially when the region of interest is as large as the Gulf Coast Region of the United States (GCR), which includes the coastal zones of Texas, Louisiana, Mississippi, Alabama, and Florida. Many datasets that speak to the ecological and socioeconomic benefits of landscapes do not have continuous or consistent coverage across the GCR. All the data from each Gulf Coast state must be combined and analyzed to make something meaningful of the numbers—an immense task. This is the main goal of the Conservation Prioritization Tool (CPT). The CPT is a conservation planning software being developed by the Strategic Conservation Assessment of Gulf Coast Landscapes (SCA) Project. The SCA Project's main objective is to create a framework for assessing the value of conserving lands within the Gulf Coast Region (GCR) based on multiple ecological and socioeconomic criteria, called data measures.

There are 21 data measures currently in the CPT (Shamaskin et al. 2019), three of which we developed during the summer of 2020: 1) Riparian Buffer Land Use/Land Cover (LULC), 2) FloodplainConnectivity, and 3) Invasive Plants Suitability. Developing these data measures provides fulfillment of data gaps and inconsistencies that exist in the gulf-wide data. These data gaps refer to data that either do not exist, lack consistent spatial coverage or lack consistent approaches in generating data. Aggregating state data in the Gulf Coast Region is one way to bridge these data gaps, and it is the method we used for these three measures. By filling data gaps and reconfiguring inconsistent data, this work provides more ecological and socioeconomic evidence to help guide land conservation actions throughout the GCR. For instance, providing these data measures to decision-makers in land conservation helps to preserve or restore water quality and connectivity on the landscape and predict areas of high invasive plant species concentration.

Water quality has increasingly become a concern over the past two decades of ecological literature. The main issue is poor water quality due to nutrient runoff from anthropogenic land uses like agriculture and urban developments. This makes knowing what land cover is within 100 meters of water important for land conservation. In the Riparian Buffer LULC data measure, we focus on the land uses/land covers present within 100 meters of either side of streams and rivers across the GCR. These 100-meter areas along both sides of streams are called riparian buffer zones, and they are ecologically important as they "are effective in reducing the nutrient concentrations in water that pass through them" (Venkatachalam et al. 2004). Natural lands like forests, shrubland, and grasslands are preferred riparian buffer land covers because the vegetation filters the water instead of adding nutrients to the water like agricultural sites within the buffer zone do (Venkatachalam et al. 2004). Riparian Buffer LULC quantifies the amount of natural lands relative to anthropogenic lands within the riparian zone of a waterbody; this proportion directly informs the quality of the riparian buffer.

Floodplains are defined as "areas of low-lying land that are subject to inundation by lateral overflow water from rivers or lakes with which they are associated" (Junk & Welcomme 1990). We are interested in floodplain connectivity, which describes the waterflow between floodplains and their rivers or lakes. An important role of floodplain connectivity is "driving species composition and richness in riparian ecosystems by offering the exchange of nutrients, sediments and organic matter as well as biotic elements such as plant dispersal units" (Leyer 2006). Unfortunately, with the implementation of levees, dams, and roadways between rivers and floodplains, people have altered the hydrology of these systems and in turn disrupted this exchange; this negatively affects the usefulness and value of these landscapes for conservation (Tockner and Stanford 2002). In the Floodplain Connectivity measure, we quantify how connected the floodplain is with its associated waterbody, which is determined by the amount of floodplain area that is free of anthropogenic obstructions to its associated waterbody.

The last data measure is Invasive Species Suitability, which indicates the probability of invasion from different nonnative plants that pose ecological and economic impacts to the GCR. Many people in the south east U.S. are familiar with highly invasive species like kudzu and Japanese honeysuckle, but according to Lázaro-Lobo et al. (2020), there are 45 species considered worthy of determining risk of invasion within the south east US. This is significant because invasive plant species threaten the success of native plant species that supply food and shelter for wildlife. Knowing where these invasive species are likely to occur enables wildlife conservationists to plan accordingly to combat these species in order to conserve the wildlife that depends on the abundance of native plant species.

Methods and Data

Riparian LULC

The main objective of this data measure is to quantify the amount of land-uses/land-covers (LULCs) of riparian buffers, which we defined as 100-meter buffers from all streams, in the SCA region. We used eight data sources to define this measure: 1) four csv datasets each describing one of the four Gulf Coast riparian buffer regions 03S, 03W, 08, and 12 (NHDPlus 2020) and 2) four shapefiles of NHDPlusV2 flowlines for the aforementioned regions (USEPA 2020).

We used the following R packages to process these files: sp, ggplot2, rgdal, tidyr, diplyr, sf, leaflet, reshape2, raster, rgeos and maptools (Cheng et al. 2019). Each riparian buffer region dataset reports its stream segments (each identified by a multidigit numeric code, called its COMID), and by these stream segments, the dataset reports catchment and watershed areas (square km) as well as the percentages of area classified by LULC, all within a 100-m buffer of NHD streams. We focused on only catchment data for the following LULCs: wetland, urban, forest, agricultural, grassland, shrub/scrub, and bare land.

We used the flowline datasets, cropped to the SCA region in ArcGIS (ESRI 2019), as SpatialLinesDataFrames by which we were able to merge the riparian buffer regions together and create a dataset with all flowlines and riparian buffer LULCs for a 100-m buffer around each

flowline within the SCA region. We then calculated the total percent catchment LULCs within the SCA region (i.e. % wetlands, % urban, % forest, etc), which we used to calculate the total area (square km) of each LULC.

Floodplain Connectivity

The main objective of this measure is to delineate connected floodplains within the SCA region. We classified floodplains as EPA 100-year floodplains. We used three raster data sources to define this measure: 1) a raster layer showing the relative inundation frequency (IF) of the GCR landscape (Allen 2016), 2) NOAA high tide extent (accessed July 20, 2020) and 3) the EPA 100-year floodplain (USEPA 2018).

We used the following R packages to process these files: raster, rgdal, ggplot2, and sp. The IF dataset reports a relative inundation frequency index from 0 - 100 and depicts typical seasonal flooding across the SE Region (Allen 2016). We used the entire IF dataset extent - excluding extreme (low frequency) observations of inundation indices of <5. Since the optical remote sensing approach used by Allen (2016) has documented limitations in areas of dense vegetation such as coastal marshes, we supplemented this layer with the NOAA high tide layer. We noted errors in the EPA high tide flooding layer in low lying areas in south Louisiana (e.g. New Orleans). These errors were partially corrected by applying a mask to flooding extent within urban areas. The combination of these two raster layers defines an improved measure of the area of typical seasonal flooding extent in coastal and riverine floodplains. We cropped the combined layer to the SCA region in ArcGIS (ESRI 2019).

We used the EPA 100 year floodplain extent (USEPA 2018) as the superset of all potential floodplain area. We cropped the EPA floodplain layer to the SCA region in ArcGIS and reclassified its values from 0 and 1 to 0 and 2 with the reclassify() function in R.

Finally, we overlaid the layer of typical seasonal flooding with the EPA 100 year floodplain using the "overlay analysis" function in ArcGIS to identify floodplain areas that are connected (and typically inundated) and floodplain areas that are disconnected (and typically dry).

Invasive Species Suitability

The objective of this measure is to determine the probability of invasion from different nonnative plants within the SCA region. Our data is from Adrián Lázaro-Lobo, a PhD in the Biology department of Mississippi State University, who developed probability of invasion maps for 45 nonnative species within the Southeast United States (Lázaro-Lobo et al. 2020).

Using species distribution maps from EDD Maps, we determined 31 of Lázaro-Lobo's invasive species lie within the SCA region. We then used ArcMaps (ESRI 2019) to 1) clip each of the 31 probability of invasion maps to the SCA region and 2) average each species' probability to create an index of probability of invasion. Because very few of these species are listed as state and federal noxious weeds although we know them to be noxious, we decided not to weigh certain species. We incorporated the unweighted index into the 1 km^2 hexagons of the SCA region.

Results

We found natural lands comprise >78% of land cover within riparian buffer zones in the GCR. This supports the notion that water quality of these associated streams may be enhanced by the presence of nearby natural lands. We designated tiers to group each LULC. Anthropogenic riparian buffers can easily be seen through the maps in Figure 1, as well as areas with relatively high natural land. Undesirable regions for conservation based on riparian buffer LULC are colored dark red.

Additionally, Figure 2 shows there is connectivity along coastal floodplains, except those that are part of Houston and Tallahassee, with poorer connectivity moving inland for all states within the SCA region. Louisiana has the best connectivity along its coast, with southern Florida following. The data indicate that the floodplains like the Mississippi River, Pascagoula River, Florida Everglades, Tensaw River, coastal Texas, and coastal Louisiana are well connected.

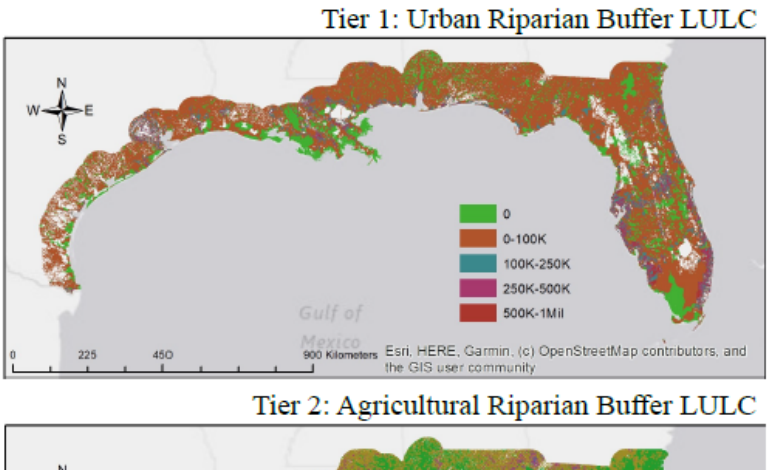

Figure 1 Riparian Buffer Tier Maps show LULCs across the SCA region. Note areas in dark red, which represent areas of a conservationist would not want to conserve based on riparian buffer LULC. These are large urban and agricultural sites as well as low natural cover type sites.

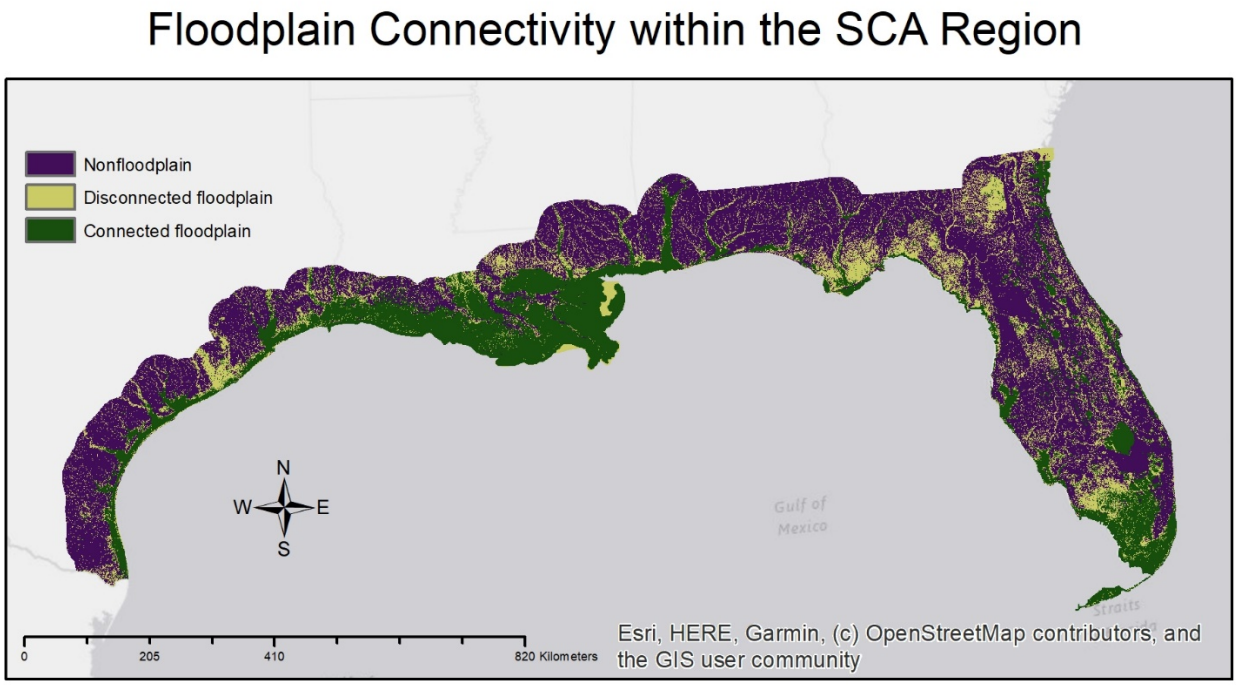

Figure 2 Floodplain connectivity in the SCA region. Note the disconnected floodplains around Houston, New Orleans, and Tallahassee are atypical of the trend for connectivity along the coasts. This demonstrates the effects of floodplain draining, levees, and altered hydrology in urban areas.

Lastly, our data demonstrate the highest probability of invasion in the SCA is 0.7. Each state mostly has low probabilities of invasion across the landscape, yet nonnative species seem to be highly likely to invade Houston, Texas and central Florida.

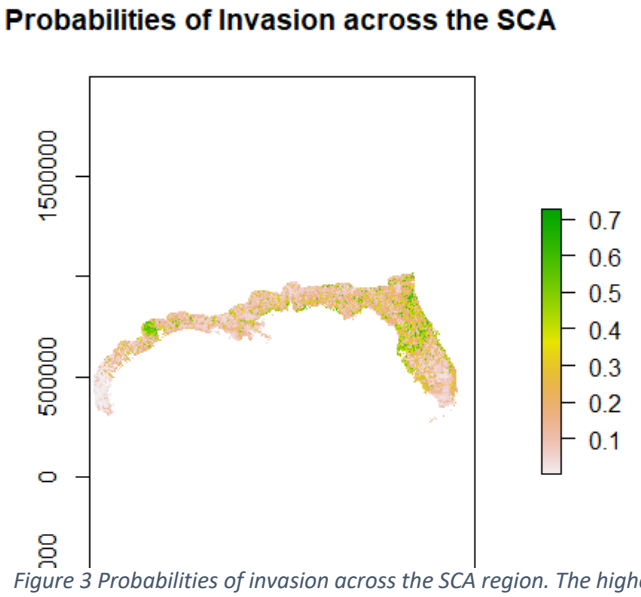

Figure 3 Probabilities of invasion across the SCA region. The highest probabilities occur in each state, but they are mostly concentrated around Houston, TX and central FL.

Discussion

Riparian Buffer LULC

Although our data indicate riparian buffer zones in the SCA are mostly natural lands, forest and wetland riparian buffers are under threat from anthropogenic developments (Burton 2005). With this concern in mind, a decision-maker may choose to conserve these limited forest riparian buffers.

We defined riparian buffers as the EPA does, 100-meter zones from all streams, but it may be the case that some streams do not require the full 100 meters while others require more. Therefore, an adaptive approach to riparian zone size may be the best option in future. This kind of process would consider multiple criteria of the riparian area for the most likely size of the buffer zone.

Floodplain Connectivity

The inundation frequency we used in this measure under-reported inundation rates around coastal areas due to cloud cover often blocking the satellite images form accurately detecting inundation in these areas. As a result, the layer showed coastal cities, like New Orleans as frequently inundated, but since the city is protected by levees, it should not be part of the floodplain even though it does flood a lot. To address this issue, we applied a mask onto the original layer from NOAA Mean-Higher-High-Tide layer so that it captures coastal areas and excludes New Orleans and other coastal cities from inundation (NOAA).

We utilized 100-year floodplain data in this tool, but there are narrower floodplain definitions that would restrict the floodplain size and therefore the connectivity. It may be the case that using all areas that have a 1 in 100 chance of flooding every year includes too much area that is actually not critical to the floodplain even though it technically has a chance of flooding. Nonetheless, we included even the areas with a 1% chance of flooding each year to paint the full picture of floodplains within the SCA region.

Invasive Species Suitability

Although nonnative species have potential to become invasive, it is important to understand that not all nonnative species will. A species' invasiveness depends on qualities like its ability to survive, reproduce, and outcompete other species in a habitat. Usually, outcompeting other species is what makes an invasive species so successful in establishing monocultures, or stands of only the invasive species. Other nonnative species may be less aggressive and be able to coexist with native species. These docile species are not a concern for the Invasive Species Suitability measure in the CPT. The 31 species in this measure are likely to be invasive in the habitats they can survive in.

So far, the CPT does not tell which species are likely to invade a given area. Although an ecologist may already know what species are invasive in ecosystems (i.e., water hyacinths and giant reeds in wetlands, kudzu in forests, Chinese tallowtree in bottomland forests, etc.), the CPT could better inform the ecologist that certain species are likely to invade the area of interest for conservation. This is because, again, some species are more aggressive than others and therefore much more difficult and expensive to manage.

CPT Tool and Conservation

All three of these data measures are valuable to land conservation. Anyone in charge of deciding what land is best for conservation for his/her purpose will need to know the quality of any riparian buffer zones in the area, as well as whether the area is within a floodplain (connected or disconnected, if so), and the probability that invasive species will occupy the area during their management. For example, anyone interested in conserving secretive marsh birds in southeast Louisiana would be interested in high quality riparian buffers, connected floodplains, and low

probabilities of invasive plant species outcompeting necessary native plants for habitat and food. It is also likely that no site will be absolutely perfect for this purpose, so the decision-maker would need to weigh the benefits to the costs of potentially restoring a site.

The CPT helps decision-makers easily compare sites within the SCA by filling data gaps across the region for each data measure and by providing easy access to each data measure pertinent to conservation. By simply selecting or drawing an area in the SCA region, anyone can see data for 21 economic and socioeconomic factors, which can then be used to compare the values for multiple areas. This allows decision-makers to choose the best site for their goals.

Conclusion

Land conservation decisions entail a longer list of factors besides these three data measures only. The CPT covers 21 various ecological and socioeconomic factors, including threatened and endangered species (number of species and critical habitat area percentage), connectivity to existing protected area, and biodiversity index. The full tool suite guides land conservation in the U.S. Gulf of Mexico Coastal Region.

Sources Cited

Allen, Y (2016) Landscape Scale Assessment of Floodplain Inundation Frequency Using Landsat Imagery. River Research and Applications 32:1609–1620.

Burton ML, Samuelson LJ, Pan S (2005) Riparian woody plant diversity and forest structure along an urban-rural gradient. *Urban Ecosyst* 8**:**93–106

Cheng J, Karambelkar B, and Xie Y (2019) Leaflet: Create interactive web maps with the Javascript "Leaflet" library. Open Source R Package.

ESRI (2019) ArcGIS Desktop. Environmental Systems Research Institute, Redlands, California.

Junk WJ & Welcomme RL (1990) Floodplains. In: *Wetlands and Shallow Continental Water Bodies,* ed. B.C. Patten *et al*., pp. 491–524. The Hague, The Netherlands: SPB Academic Publishers.

Lázaro-Lobo A, Evans KO, and Ervin GN (2020) Evaluating landscape characteristics of predicted hotspots for plant invasions. Invasive Plant Science and Management. doi: 10.1017/inp.2020.21

Leyer I (2006) Dispersal, diversity and distribution patterns in pioneer vegetation: The role of river-floodplain connectivity. Journal of Vegetation Science 17:407-416

Mitsch JM, Bernal B, Hernandez ME (2015) Ecosystem services of wetlands, International Journal of Biodiversity Science, Ecosystem Services & Management 11:1-4

National Oceanic and Atmospheric Administration (NOAA) NOAA MHHW Data Map website, accessed July 20, 2020, at https://www.tidesandcurrents.noaa.gov/waterlevels.html?id=8419317&units=standard&bdate=20160131&edate=20160229&timezone=GMT&datum=MLLW&interval=m&mm=MHHW

National Hydrography Dataset Plus (NHDPlus) (2020) NHDPlusV2 Data Map website, accessed June 2020, at https://www.epa.gov/waterdata/get-nhdplus-national-hydrography-dataset-plus-data#Download

Shamaskin, A., S. Samiappan, J. Liu, J. Roberts, A. Linhoss, and K. Evans. 2019. Multi-Attribute Ecological and Socioeconomic Geodatabase for the Gulf of Mexico Coastal Region of the United States. Data 5:3.

Tockner K, & Stanford JA (2002) Review of: Riverine Flood Plains: Present State and Future Trends. Biological Sciences Faculty Publications 166

United States Environmental Protection Agency (USEPA) (2018) Estimated floodplain map for the conterminous United States. doi: 10.23719/1503085

United States Environmental Protection Agency (USEPA) (2020) NHDPlus Landscape Attributes: StreamCat, accessed June 2020, at ftp://newftp.epa.gov/EPADataCommons/ORD/NHDPlusLandscapeAttributes/StreamCat/HydroRegions/

Venkatachalam A, Radhakrishnan J, Yamaji E (2004) Impact of riparian buffer zones on water quality and associated management considerations. Ecological Engineering 24:517-523

Name: Abigail Grant
Faculty Mentor: Vincent Klink

Major: Biomedical Engineering
Department: Agricultural and Biological Engineering

Genetic Cloning and PCR Techniques aid in Discovering H. glycine Resistant Genes

Introduction

In 1954, H. glycine (soybean cyst nematode, SCN) were first identified in North Carolina and may have traveled from imported, contaminated soil samples from Asia. Over time, H. glycines have contaminated many soybean farmer's crops and have become one of the most invasive species that many North American farmers must battle.

Figure 1. An example of a soybean plant's leaves discoloration from SCN.

The symptoms that appear on soybean plants during SCN infections is chlorosis, which is the yellowing of the leaves and poor drainage through the roots. It also reduces the number of seeds that the soybeans can yield and result in a reduced ability to take the proper amount of water and minerals. Therefore, these plants become stunted, unhealthy, and almost impossible to use for production. As the number of SCN infected plants arose, the USDA took extensive measures to research this invasive disease by collecting various soybean collections and tested to determine the natural resistance to SCN.

Background

Studies have been conducted to split the trials on the soybean seeds gathered to test the resistance to SCN. These trials were variety trials that split up the resistance genes into 7 accessions that displayed resistance to SCN. These genes were further tested into 5 important resistant loci that are known as rhg1, rhg2, rhg3(Caldwell et al. 1960), rhg4, and rhg5. The desirable outcome for soybeans would have traits such as yellow seed coats, no pod shattering, and high yield count. While testing out these resistant genes, some undesirable traits were found during the testing process which is known as linkage drag which creates inconsistencies and loss of time and money when it comes to growing these soybeans.

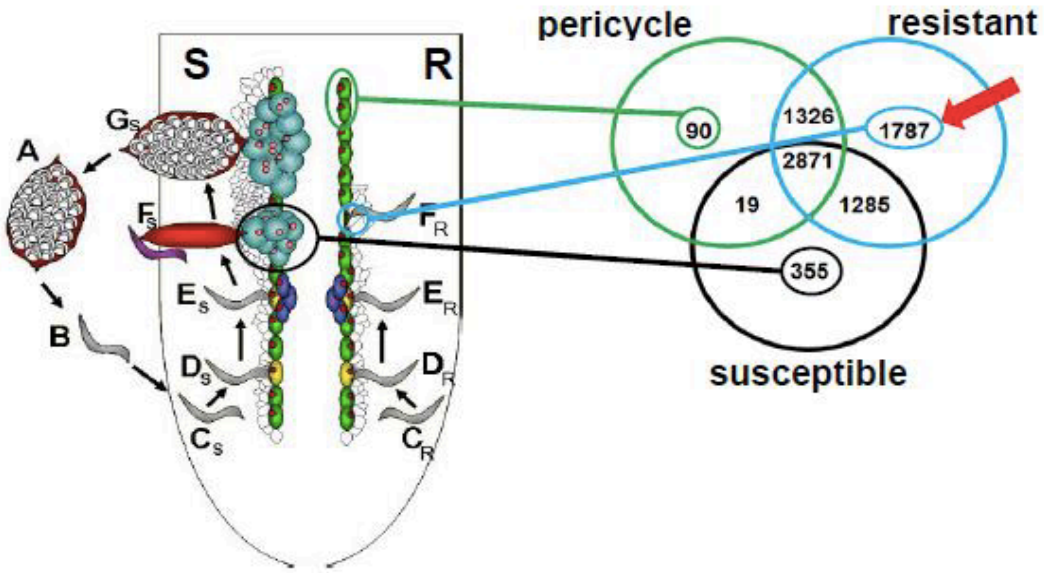

Figure 2. The candidate resistant gene identification. The left side displays the susceptible and resistant reaction to SCN and the life cycles of these genes. The right side displays the resistant gene's lifespan and how there are 1,787 resistant genes.

Over time researchers such as cell biologists have taken attention to this phenomenon to understand the processes that lead to resistance, especially with the Peking genotype and the genes that are expressed. These experiments were developed with cancer biologists with laser

microdissection to embed tissue in wax and then cut into thin sections on a rotary microtome. Then, the cells are cut out of the histological section with a laser beam for collection. After collection, the mRNA is collected and isolated to be used in various gene expression experiments such as PCR, TAQ PCR, D-TOPO cloning, LR cloning, and the culturing of the genes that are still expressed afterwards. Whenever these genes are sequenced, these specific genes can be identified and determined for understanding what specific genes can be used for farmers and scientists (Klink et al. 2015). The genes are active in the cells undergoing the process of resistance which can be hypothesized that they function as resistance genes. Therefore, these genes are candidate resistance genes which can be tested for further information as the goal of this experiment.

Materials and Methods

Six BIK resistant genes were prepared for Polymerase Chain Reaction (PCR) testing. This consisted of NF water, accuprime reaction mix, cDNA, polymerase and was tested over a period over about 2 weeks. Then after the PCR testing, the samples were injected into agarose gel with trackit orange LB and DNA ladder for the samples to move along the electron moving liquid. These samples were then taken for PCR purification where small pieces of gel that had bands on it were purified through various centrifuging steps until the remaining product was left. TAQ PCR was then done with similar techniques as normal PCR except MgCl2 and dNTP, plasmid, and forward and backward primers are added to verify if the specific genes were expressed as they were the first time. After verification, D-TOPO cloning was done with the purified solution, salt solution, and a D-TOPO vector to transform the cells into E-coli cells after several icing and centrifuging steps to shock the cells and incubate them. Afterwards, the cells were cultured and observed for any white colonies to be collected for one more TAQ PCR test.

After the cells were collected, it was transformed into agrobacterium cells by incubating the samples in liquid nitrogen for 5 minutes, ice water bath for 5 minutes, put on ice for 1 minute, and then shaken for about 3 hours. Then these were plated on LB plates and TAQ PCR was done to check the insert plasmid and regrown on plates. These stocks are utilized during a vacuum infiltration period of 15 minutes. After the co-cultivation, the vacuum is slowly released and the root-less stocks are then planted with the cut ends placed individually 2-4 cm deep into fresh, coarse, non-sterilized, vermiculite in 50-cell flats. The stocks are then transferred to the greenhouse, uncovered, and grown for 7 additional days where the roots can be observed under Dark Reader Spot Lamp fluorescent light to see if the roots were transformed.

Figure 3. The plants above are an example of a co-cultivated transformed group of soybeans that were left in the green house at this time for about 2 weeks.

Results and Discussion

Out of the 6 BIK genes, only BIK-7 and BIK-9 were utilized for the plant transformations that were done over a course of about 2 months. They were the only genes that repeatedly displayed bands at the correct regions of PCR testing and therefore were utilized for the transformations. Over a period of about 2 weeks, the plants seemed to be stable and healthy, with any fungi thrown out. However, due to the pandemic, there was a hold of time of about 2 months before the experiment could be continued. This ended in the plants dying and not being useful for examination for further testing.

Figures 4 and 5. On the left side is pictured one of the trays of transformed plants that had yellowing and almost no yield of healthy roots to use for examination. On the right picture the roots were cut for the fluorescent light testing and needed bright neon roots to display the transformed roots. This picture shows the result of the dead roots and how they do not show under this type of lighting.

Conclusions

Based on the experiments performed with PCR testing and various other genetic cloning techniques, it can be concluded that there are several genes that are useful for this experiment.

The knowledge of cell biology contributes greatly to the understanding of how various crop diseases can be understood and used to improve production for farmers and science and save millions of dollars for businesses. Even though the pandemic put a halt to the rest of the experiment after the transformations, there are many useful things to understand with genetic engineering and how important it is. As our understanding of SCN and the resistant genes are discovered, millions of dollars can be saved in the farming industry to lower costs and produce better crop yield for many.

References

1. Caldwell BE, Brim CA, Ross JP. 1960. Inheritance of resistance of soybeans to the soybean cyst nematode, Heterodera glycines. Agron J

1. Matson AL, Williams LF. 1965. Evidence of a fourth gene for resistance to the soybean cyst nematode. Crop Sci

2. Rao-Arelli AP. 1994. Inheritance of resistance to Heterodera glycines race 3 in soybean accessions. Plant Dis.

3. Klink VP, Prachi D. Matsye, Katheryn S. Lawrence and Gary W. Lawrence. 2015. Engineered Soybean Cyst Nematode Resistance.

Acoustic Levitator on a UAV

Britain Steele

Aerospace Engineering

Advisor: Dr. Zhenhua Tia

Graduate Assistant: Teng Li

Research Partner: Alston Dye

Mississippi State University, Mississippi State, MS 39762

Abstract

In the scientific community, it is known that sound can manipulate a particle's orientation. This manipulation is often used in medical practice when trying to analyze a microscopic cell without compromising or touching it. However, acoustic manipulation is being studied in engineering communities, specifically acoustic levitation. Even though there are studies about optimizing optical levitation to lift small objects, acoustic levitation still has untapped potential. The objective of this research is to test a constructed acoustic levitator's performance while it is in motion. This will be done by attaching an acoustic levitator as a payload to the bottom of a UAV. This research report contains the methodology of constructing and testing the acoustic levitator statically as the system will be tested in motion later.

Nomenclature

ARF = Acoustic Radiation Forces

CAD = Computer-Aided Design

c = Speed of Sound

p = Pressure

R = Radius of spherical trap

U = Acoustic Radiation

u = Velocity

UAV = Unmanned Aircraft Vehicle

ρ = Density

Introduction

An acoustic wave can produce an acoustic radiation force (ARF) which induces a non-pressure pocket in 3D space. This non-pressure pocket is otherwise known as the trap. For an acoustic levitator, this trap is achieved when acoustic waves oppose one another creating a standing wave in between both forces. [2] Acoustic transducers are used to produce these acoustic waves. Acoustic waves follow a sinusoidal pattern with high peaks in amplitude and large empty pockets of space in between each wavelength. For acoustic levitators, a square wave is generated electronically by an Arduino nano and amplified by a motor driver in the system's circuit. This is because square waves are easier to generate digitally than sinusoidal waves. [3] An image of the difference between a square and sinusoidal wave is shown in the image below. The blue line represents an example of a square wave, and the red line represents an example of a sinusoidal wave.

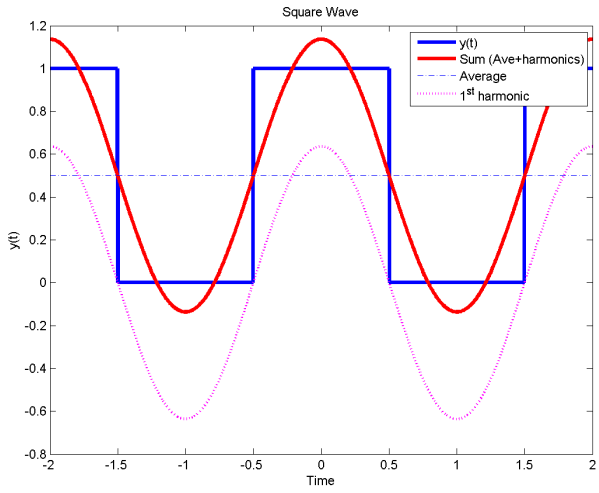

[1]

Square Wave vs. Sinusoidal Wave

Acoustic transducers are used in the system with corresponding reflectors to create a twin beam. In other words, each acoustic transducer is paired with an acoustic transducer directly across from it. To optimize the trap's sustainability, the acoustic transducers are positioned symmetrically in a conic orientation all pointing towards the center. However, the trap is constrained by Gor'kov potential in Equation 1.

$$U = 2\pi R^3 \left(\frac{\langle p^2 \rangle}{3\rho_0 c^2} f_1 - \frac{\rho_0 \langle u^2 \rangle}{2} f_2 \right) \quad \text{(Equation 1)}$$

Due to the above equation, the size of the object being sustained in levitation is limited to the size of the spherical trap. With these principles and phenomena considered, the next steps were to construct an acoustic levitator and design it to be attachable to a UAV.

Prototypes

I. Prototype 1

At the beginning of the research, we were given a zip file containing all the UAV components. For our research, we needed to analyze and gather dimensions for the bottom plate of the UAV. After doing so, my research partner and I designed our prototype using SolidWorks.

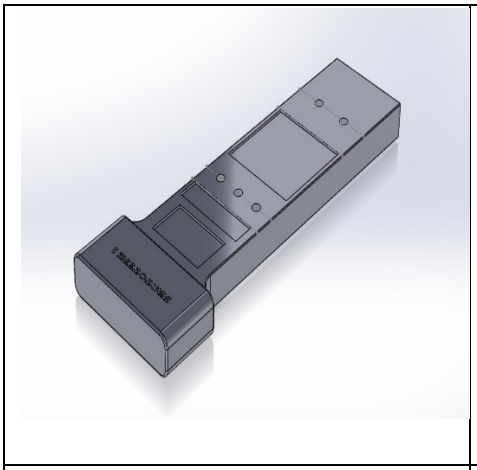	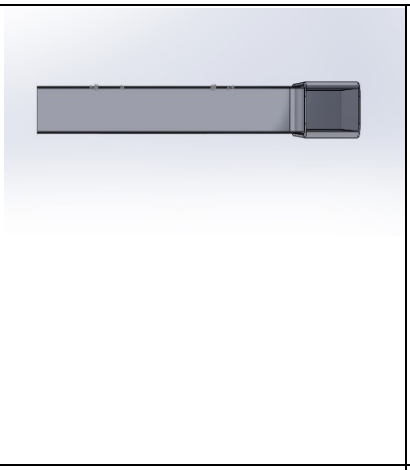	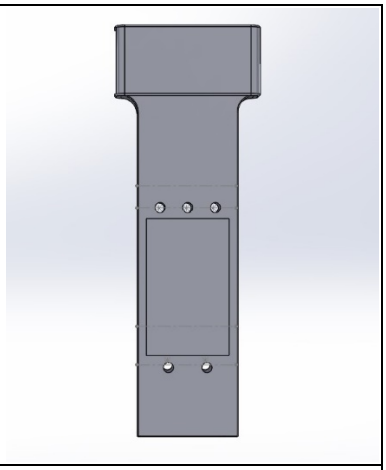
Figure A **Prototype 1, Top Isometric View**	**Figure B** **Prototype 1, Front View**	**Figure C** **Prototype 1, Bottom View**

Due to tolerance and 3D printer issues, the electrical circuit components could not fit in the designated designed slots. We mutually decided to start anew with a more efficient CAD design.

II. Prototype 2

For the second CAD design, we decided to add more tolerance and develop a design with an easier attachable feature to the UAV bottom plate.

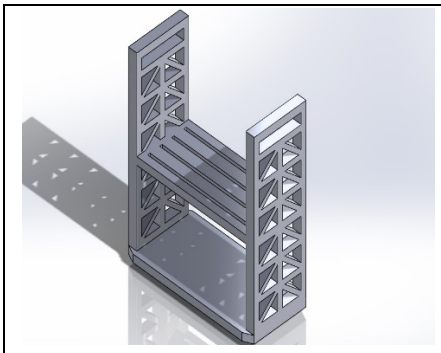	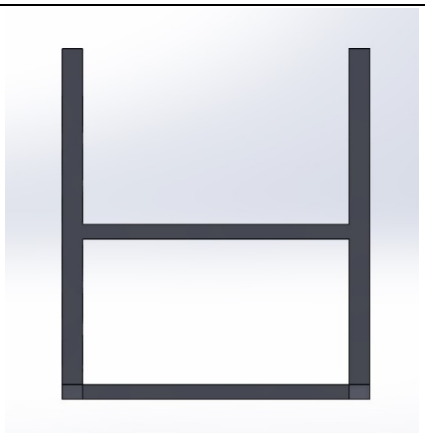	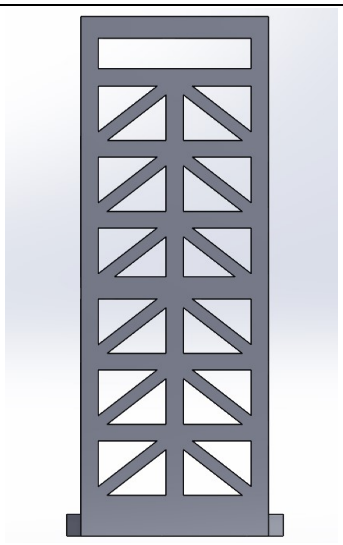
Figure D **Prototype 2, Top Isometric View**	**Figure E** **Prototype 2, Front View**	**Figure F** **Prototype 2, Side View**

This design was much more optimal. It is designed to fit all the necessary electrical components: battery, DC converter, driver, Arduino nano, and 3D printed conic structure with acoustic transducers on the inside. The 3D printed conic structure was attached with adhesive to the bottom of prototype 2, and the DC converter was placed on top of the battery with cardboard in between.

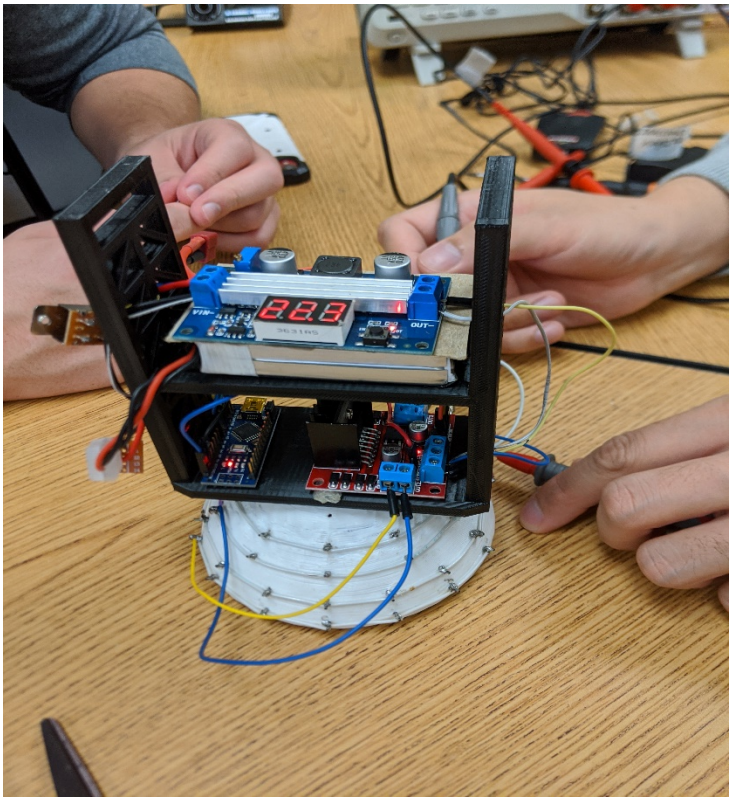

Figure G

Prototype 2, Completed Configuration

Objectives and Testing

After every part in the circuit is configured appropriately, the objectives that needed to be fulfilled were to test if the acoustic transducers were producing the correct sinusoidal waves based on frequency and amplitude, and the circuit needed to be able to handle 20V. The provided battery was faulty, so we connected another battery shown in Figure H. The array of acoustic transducers on the left are supposed to produce sinusoidal waves that have equal amplitude and frequency to their corresponding reflector. However, the reflector's wave must oscillate in an opposite direction to its counterpart. An oscilloscope was utilized to measure the amplitude and frequency of each transducer shown in Figure I. The electrical circuit was configured correctly, and each acoustic transducer array produced the appropriate sinusoidal wave.

Figure H

Replacement Battery for Static System Testing

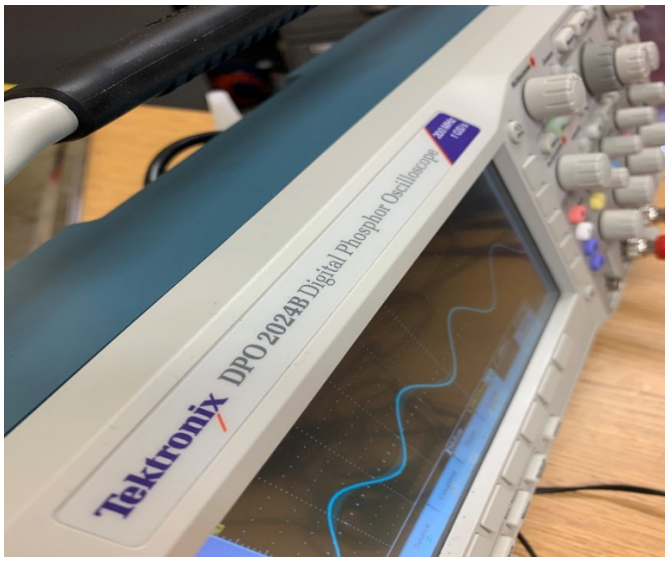

Figure I

Oscilloscope Testing for One Transducer

The next objective to complete was to prove sustained levitation in static conditions for five or more minutes. We utilized a small Styrofoam ball to represent a particle in the system. It fulfilled this objective easily. We then tested if the acoustic levitator could sustain a particle in a variety of orientations. The figures below demonstrate that all these objectives were satisfied.

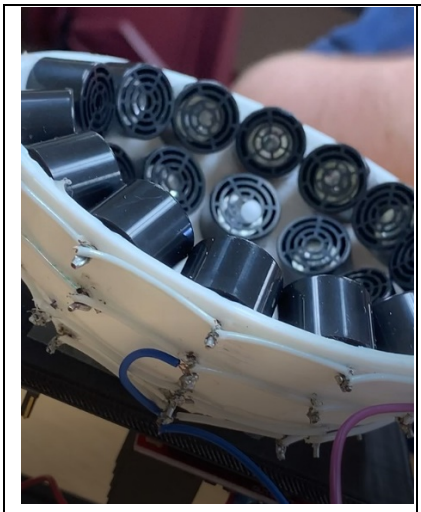	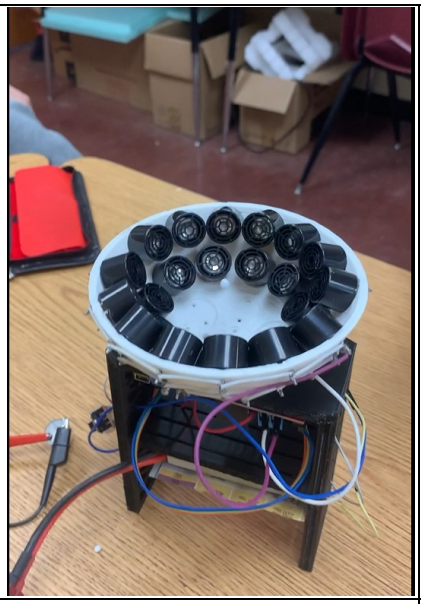	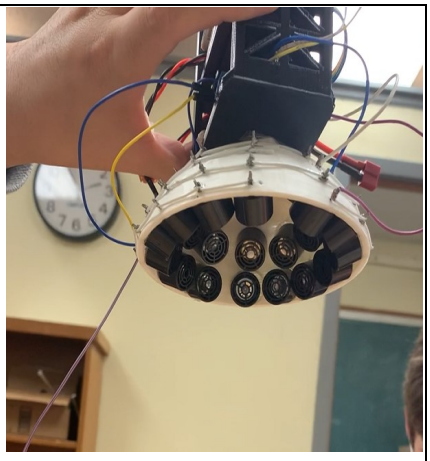
Figure J **Levitation Close-Up with Particle** **Video:**	**Figure K** **Levitation, Upward Orientation** **Video:**	**Figure L** **Levitation, Downward Orientation** **Video:**

Conclusion and Future Applications

Overall, we successfully developed an acoustic levitator. The design is optimized and ready to be attached to the UAV once we are granted access to use the UAV. The acoustic levitator configured system will be attached with either Velcro or zip ties, and we can then perform dynamic testing. It is important to note that before attaching the acoustic levitator to the UAV that a strong enough portable battery needs to be securely fastened to the system. It is also interesting that the particle stayed in the trap when we moved the system gyroscopically.

If this system were to be tested more thoroughly, acoustic levitators could be used for a variety of reasons. For the medical field, microscopic cells and particles can be more easily transportable between two sites. For the aerospace engineering community, drone product linguistics can be made more efficient. It could also have military applications as acoustic levitators allow a user to pick up an object without touching it.

Acknowledgments

I want to first thank Dr. Zhenhua Tia for providing me the opportunity to participate in his research. I have learned so much valuable information as this is my first research report. It was initially a daunting task, but for the Fall 2020 semester, I felt that I developed more as an aerospace engineer. Secondly, I want to thank Teng Li and Alston Dye. These two individuals were vital components in the success of this research project. As I am a younger individual, they demonstrated traits that I aspire to have in my future collegiate careers. They were dedicated as much as I was to complete this research project, and for that, I could not be more thankful.

References

[1]

Erik Cheever, S. C. Fourier Series Printable. Linear Physical Systems - Erik Cheever Available at: https://lpsa.swarthmore.edu/Fourier/Series/FSAll.html. (Accessed: 17th January 2021)

[2]

Marzo, A. *et al.* Holographic acoustic elements for manipulation of levitated objects. *Nature News* (2015). Available at: https://www.nature.com/articles/ncomms9661. (Accessed: 17th January 2021)

[3]

Marzo, A., Barnes, A. & Drinkwater, B. W. TinyLev: A multi-emitter single-axis acoustic levitator. *AIP Publishing* (1970). Available at: https://aip.scitation.org/doi/10.1063/1.4989995. (Accessed: 17th January 2021)